Greedy copula segmentation of multivariate non-stationary time series for climate change adaptation



Taemin Heo, Lance Manuel

PII: S2590-0617(22)00008-4

DOI: https://doi.org/10.1016/j.pdisas.2022.100221

Reference: PDISAS 100221

To appear in: Progress in Disaster Science

Received date: 31 July 2021

Revised date: 24 February 2022

Accepted date: 27 February 2022

Please cite this article as: T. Heo and L. Manuel, Greedy copula segmentation of multivariate non-stationary time series for climate change adaptation, *Progress in Disaster Science* (2021), https://doi.org/10.1016/j.pdisas.2022.100221

This is a PDF file of an article that has undergone enhancements after acceptance, such as the addition of a cover page and metadata, and formatting for readability, but it is not yet the definitive version of record. This version will undergo additional copyediting, typesetting and review before it is published in its final form, but we are providing this version to give early visibility of the article. Please note that, during the production process, errors may be discovered which could affect the content, and all legal disclaimers that apply to the journal pertain.

© 2022 Published by Elsevier Ltd.

Greedy Copula Segmentation of Multivariate Non-Stationary Time Series for Climate Change Adaptation

Taemin Heo^{1*}, Lance Manuel^{1†}

¹Department of Civil, Architectural and Environmental Engineering
The University of Texas at Austin, 301 E Dean Keeton St C1700, Austin, TX, USA, 78712

*Corresponding Author: taemin@utexas.edu; †lmanuel@mail.utexas.edu

Acknowledgements

This material is based upon work supported by the National Science Foundation under Grant No. CMMI-1663044. The authors are grateful for this support. Any opinions, findings, and conclusions or recommendations expressed in this material are those of the authors and do not necessarily reflect the views of the National Science Foundation.

Greedy Copula Segmentation of Multivariate Non-Stationary Time Series for Climate Change Adaptation

Abstract

Non-stationary climate data are often encountered in dealing with natural hazards, climate change and disaster reduction. With drought, for instance, it is common to encounter such non-stationary data sets (time series). The objectives of this work are to formulate a rational data-driven approach that can consider non-stationary and time series on multiple random variables that can have generalized underlying probability distributions and dependence structures. The methodology proposed seeks to divide up the data into non-overlapping segments, each of which is treated as stationary with some underlying probability and dependence structure, while the long time series yields multiple such segments that are mutually independent. The Greedy Copula Segmentation (GCS) algorithm developed employs best-fit probability distributions and copula function. Siter data-driven time series segmentation. Validation of the proposed methodology is demonstrated using a benchmark problem as well as a single-site realistic drought example. The proposed GCS approach has potential use in climate change adaptation (CCA) and disaster risk reduction (DRR) for any climate-related hazards involving non-stationary time series data.

Keywords: time series segmentation; greedy algorithm, non-stationary stochastic process

1. Introduction

Droughts, characterized by water shortages or a lack of precipitation and dry weather, can occur in virtually all climatic zones and can cause severe damage to the ecology and economy of regions where they occur (Mishra and Singh 2010; Yoo et al., 2013; Carrao et al. 2016; Schwalm et al. 2017; Sinch et al. 2021). Droughts can have slow onsets and they can be frequent as well as long-lasting. Lee et al., 2020's review of the international disaster database indicates that over 3.0c0 floods and droughts occurred globally from 2001 to 2018, accounting for nearly 45% c. disasters stemming from natural hazards. One chronic drought-prone state in India—Gujarat—has experienced drought almost every year for the last 35 years (Bandyopadh, a) et al. 2020). Lee et al. (2020) point out that floods and droughts caused more seve a damage in the period from 2001 to 2018 than over the entire 20th century. Secondary damage to the economy arising due to droughts can also be considerable. Worldwide, 83% of agricultural loss and damage between 2006 and 2016 were attributed to droughts; these losses amounted to over 29 billion USD (Walz et al. 2020). The Sendai Framework for Disaster Risk Reduction (SFDRR) has emphasized global disaster risk strategies that consider innovations in science and technology, but there still has not been sufficient progress in risk reduction in several sectors due to gaps in the connection of science, technology, policymaking, and climate change with evolving humankind and living patterns and societies (Djalante and Lassa 2019; Ishiwatari and Surjan 2019; Saja et al. 2019; Ishiwatari and Surjan 2019; Izumi et al. 2019; Matsuoka and Rocha 2021; Patel et al. 2021; Uchiyama et al. 2021; Wilkins et al. 2021). With droughts, especially, their unique and non-stationary characteristics make risk reduction endeavors quite challenging. An improved understanding and statistical/numerical modelling of drought patterns is vital for sustainable development in many parts of the world.

Climate data such as precipitation, wind speed, etc. make up a fundamental source of information for the risk assessment of any civil infrastructure system. Often, the climate parameter is represented as a stationary stochastic process, which then implies that the risk assessment makes use of all the available historical data in prediction. Temporal patterns

that include extreme climate events such as droughts, floods, storms, etc. can be quite variable due to inherent non-stationary characteristics and as an outcome of human-induced climate change (Lee and Ouarda, 2010; Sheffield et al., 2012; Dai, 2013; Garcia Galiano et al., 2015; Li et al., 2015; Cid et al., 2016; Van Loon et al., 2016; Ouarda and Charron, 2018; Liu, S. et al., 2019; Slater et al., 2020). Such changing patterns highlight the possible incompatibility of traditional stationary assumptions, especially when dealing with climate change adaptation (CCA).

Two branches of methods have been studied during the last decades to incorporate non-stationarity in risk assessments: 1) partitioning the time series into segments where stationary models are used to explain each segment; and 2) modelling non-stationary behaviour by introducing explanatory variables using smooth functions. The first option involves change-point detection based on Bayesian inference, hypothesis testing, and hidden Markov models, all of which seek to uncover break points in the time series data (see Reeves et al., 2007; Esling and Agon, 2012; Polunche ko and Tartakovsky, 2012; Aminikhanghahi and Cook, 2017; Truong et al., 2020 for a corporehensive survey). Such time series segmentation algorithms suffer from high computational demand especially for long time series, since finding appropriate break points is a combinatorial optimization problem that requires evaluations whose number thus grows exponentially with the number of observations. Some segmentation algorithms, as a result, are inefficient for optimizing CCA that requires planning for futures on the scale of decades based on collected hourly to monthly climate data.

The Generalized Additive Model for Location, scale, and Shape (GAMLSS) proposed by Rigby and Stasinopoulos (2005) has received agnificant attention and falls under the second class of methods (Wang et al. 2015, Cahanzaib et al. 2020, Jehanzaib et al. 2021). GAMLSS has been successfully applied for analyses in hydrology applications due to its great flexibility in addressing non-stational, characteristics. GAMLSS can, however, predict response variable trends, only when the explanatory variables can be predicted independently. Climate variables are often inter-dependent; this makes it hard to identify governing explanatory variables using CAMLSS that can then be used to arrive at optimized CCA efforts.

Recently, Hallac et al. (2012) proposed Greedy Gaussian segmentation (GGS) that addresses noted challenges in time series segmentation by identifying optimal break points using a -greedy" but approximate approach. This method lightens the computation demand involved in segmentatio to where evaluations required are reduced to varying linearly with the number of observations. Moreover, underlying assumptions with GGS and the associated formulation are better suited to CCA compared to what results with other segmentation methods. GGS assumes non-repeatability of segments unlike ergodic hidden Markov models (Rydén et al. 1998; Nystrup et al. 2017); this means that model parameters for each segment are unrelated to parameters in other segments. Considering that we are dealing with climate conditions that are widely acknowledged to be changing, the nonrepeatability assumption is justified. Also, GGS formulates the time series partitioning problem based on the maximum log-likelihood of the data. Since we are assuming piecewise stationarity and wish to project future patterns based on recent observations, a maximum log-likelihood based approach is most appropriate for our problem. One drawback of GGS is its Gaussian assumption, which is not always appropriate for climate-related problems where variables often follow non-Gaussian distributions (Zelenhasic and Salvai, 1987; Mathier et al., 1992; Yue et al., 1999; Shiau and Shen 2001; Yue 2001; De Michele and Salvadori 2003; Hao and Singh 2013; Mazdiyasni et al. 2019).

We, therefore, extend the applicability and generality of GGS by replacing the multivariate Gaussian distribution assumption with a multivariate copula choice. We refer to our approach as the greedy copula segmentation (GCS) algorithm. The use of multivariate

copulas can help to represent many complex multivariate dependence structures both by employing various options for marginal distributions and by selecting different copula families (Saklar, 1959; Salvadori, 2004; Salvadori and De Michele, 2004; Nelsen, 2006; Genest and Favre, 2007, Jehanzaib et al. 2021). Moreover, most common marginal distribution parameters can be empirically obtained from data using maximum likelihood estimation (MLE). The copula family parameter can also be non-parametrically estimated using the empirical Kendall's rank correlation coefficient, tau (Genest et al. 2011, Manuel et al. 2018). For these reasons, we propose the use of a more versatile GCS approach, while not losing advantages of the mathematical tractability of GGS.

GCS considers the non-stationary characteristics of the underlying climate process by defining sub-segments that are each stationary but mutually independent. Near-future patterns are reasonably assumed to be most similar to the most recent sub-segments. Consequently, a model derived from such recent data might be expected to lead to better predictions than what we get with the traditional approach hat uses the entire historical sample. For civil infrastructure systems, we can effectively adopt an adaptation policy based on the proposed GCS approach. A 5- to 10-year cycle of cli nate data that possibly involves policy amendment (CCA) usually starts by updating the cite specific hazard data. Then, derivative policies are updated accordingly. The projec ed risk assessment is best suited only for a near-future period because, after this period the policy will need to be amended with any newly discovered information/data. We dem.o. suate how to employ such new data along with all the available historical data to update comporal hazard patterns and derivative policies. Again, in light of the most recent climate charge trends, dated data are unlikely to contain meaningful information for near-future or jections. In fact, the use of old data can cause a model to exhibit greater bias and uncartainty due to heterogeneity in the data due to non-stationary character. By using the purposed GCS-identified optimal data, we rely on only informative recent data to update policies. In other words, GCS-CCA discards outdated data to improve prediction performance. It works more discriminately to detect and account for short-term climate abnormalities.

In this study, we make the following contributions: 1) we derive an extension of Greedy Gaussian Segmentation (Hallac et al., 2019) for use with non-Gaussian climate data and any generalized copula model: 2, we demonstrate our GCS method's possible use in plans for optimal climate change adartation; and 3) we present realistic experiments that illustrate how a near-future pattern of extreme climate events can be optimally predicted using the proposed approach. The objectives of this work are to formulate a rational data-driven approach (GCS) that can consider non-stationary and time series on multiple random variables that can have generalized underlying probability distributions and dependence structures. The proposed GCS approach has potential use in climate change adaptation (CCA) and disaster risk reduction (DRR) for any climate-related hazards involving non-stationary time series data.

To demonstrate steps in the algorithms for GCS and GCS-CCA, an example analysis on a benchmark data set is first presented in Section 2. A real-world application for drought risk assessment follows in Section 3. Discussions and conclusions follow at the end.

2. Methodology

2.1 Greedy Copula Segmentation

Assume we have bivariate climate data, available as time series data, as shown in Figure 1. Without loss of generality, assume that the time series are given at discrete data index values as shown.

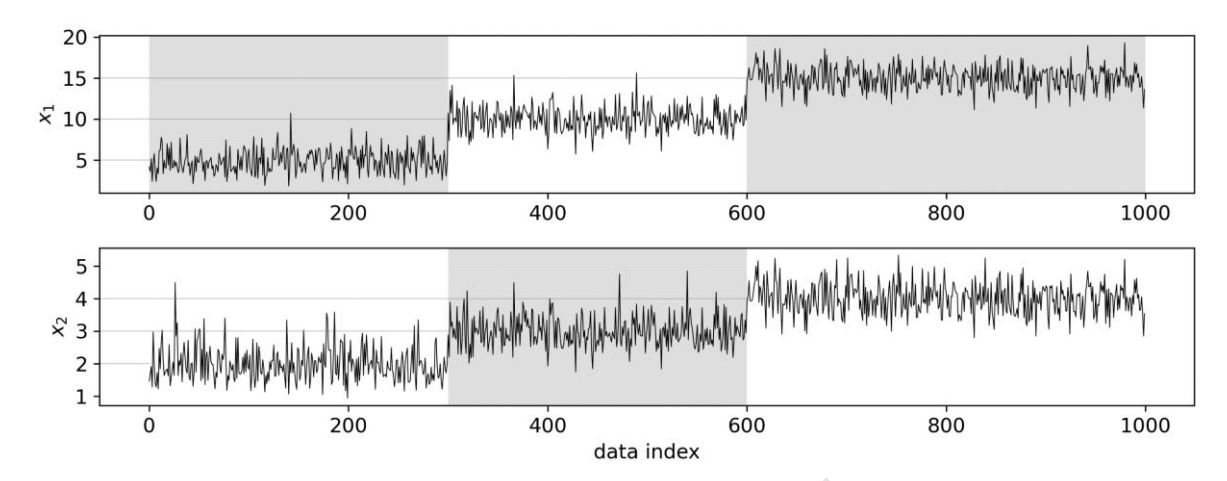


Figure 1. A realization of synthetic bivariate benchmark data 'ine series: 3 separate data segments generated using 3 different parameter settings are highlighted.

In the synthetic data selected for this example, we have the commate-related variables that follow gamma and lognormal distributions, respectively. Their dependence structure is assumed to be represented by a Clayton copula. A total or 1,000 samples were generated with 3 different parameter settings to embed non-stationary character in the data. We have 5 parameters to define the two variables in each or the 3 subsets—they include a copula parameter, α ; parameters describing the shape, a, and scale, b, for the gamma variable; and the mean, μ , and standard deviation, σ , for the lognormal variable. Note that the mean and variance of the gamma variable are ab and al^2 , expectively.

For the data, the first 300 samples are synthetically generated using $\Theta_1=(\alpha,a,b,\mu,\sigma)=(1,10,0.5,2,0.5)$, the next 300 samples use $\mathcal{O}_1=(10,40,0.25,3,0.5)$, and the final 400 samples are from $\Theta_3=(50,100,0.15,4,0.5)$. For the gamma-distributed variables, the different parameter settings are equivalent to seeing different mean values of 5, 10, and 15, and variances of 2.5, 2.5, and 2.25. Figure 2 shows copulas according to the different parameter setting selections. As is clear from Figure 1, the generated time series are non-stationary; the values of both variables are seen to get higher with time (increasing data index value). As such, this synthetic bivariate climate benchmark data set could represent changing extreme climate events — such as storms, floods, droughts, etc. — that get more frequent and severe with time.

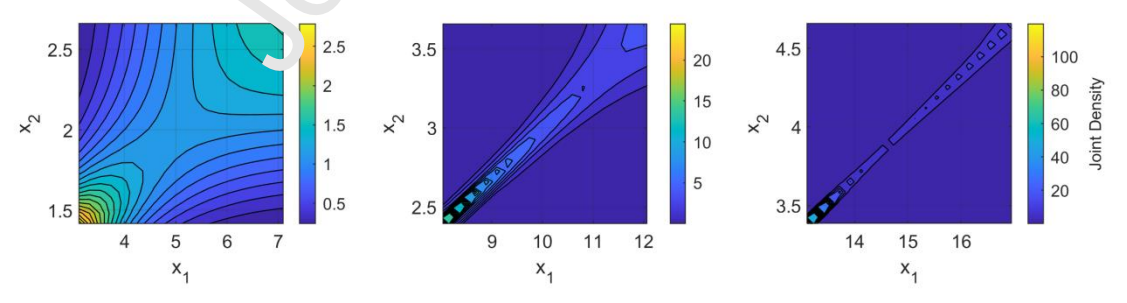


Figure 2. Copulas for the synthetic benchmark data generation using θ_1 , θ_2 , and θ_3 (left to right).

From the above, one might expect that near-future patterns are most likely to be similar to the last 400 samples. The earlier 600 samples are likely to be deemed outdated and would increase uncertainty in any near-future prediction. Our goal is to find and uncover the last stationary sub-segment from the data. To achieve this goal, we iterate the greedy

segmentation approach until no further segmentation on the last segment offers any advantage.

2.1.1 Iteration 1

The GCS algorithm starts with the benchmark data that can be denoted as $X = [\mathbf{x}_1, ..., \mathbf{x}_{1,000}]^T$, where $\mathbf{x}_i = (x_1(i), x_2(i))$. Also, $x_1(i)$ and $x_2(i)$ represent the ith index values of the first and the second variable, respectively. Note that \mathbf{x}_i represents a 2-dimensional vector containing these ith index values of both variables and X represents the entire bivariate data set.

We consider the data as a segment and, thus, the number of current segments K=1; by splitting the data into more segments, the value of K will be changed. In every GCS iteration, we will consider a new breakpoint that then divides one of the current segments into two sub-segments. In the first iteration, we have 999 possible sew breakpoints denoted as $b_{1\backslash 2}, b_{2\backslash 3}, \ldots, b_{999\backslash 1,000}$, where the location of a breakpoint is indicated by the subscript. For instance, $b_{k\backslash k+1}$ is a breakpoint that divides the data into two sub-segments $X_1=[\mathbf{x}_1,\ldots,\mathbf{x}_k]^T$ and $X_2=\begin{bmatrix}\mathbf{x}_{k+1},\ldots,\mathbf{x}_{1,000}\end{bmatrix}^T$. Figure 3 shows an example with $b_{k\backslash k+1}$, where k=500.

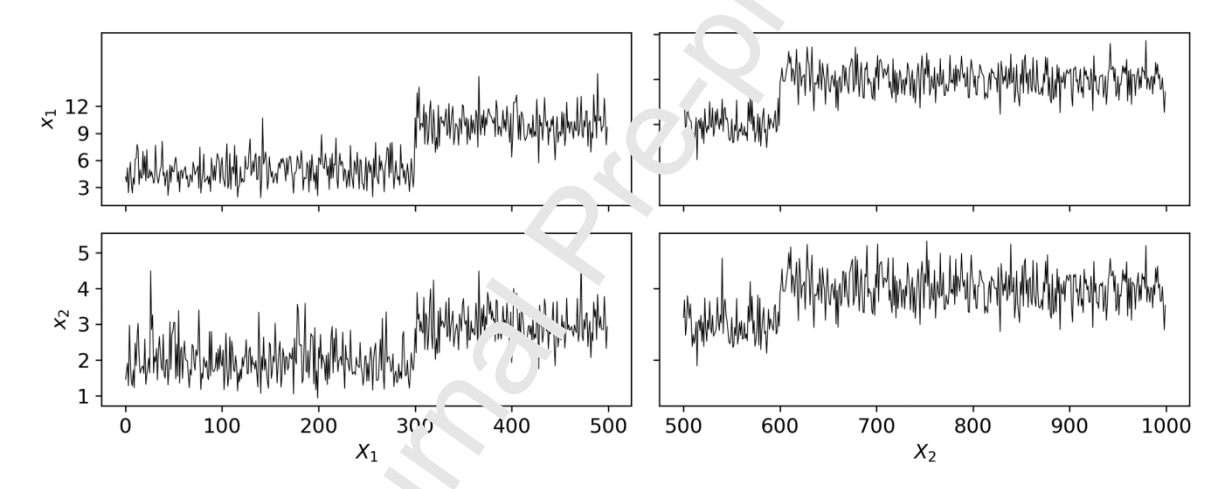


Figure 3. Example sub-segments generated by breakpoint, $b_{500\setminus501}$.

Next, we compare two scenarios: 1) where X represents independent bivariate samples from a multivariate copula \mathcal{C}_{Θ} based on all the data; and 2) where X_1 and X_2 represent separate bivariate samples from two different copulas, $\mathcal{C}_{\Theta_{(1)}}$ and $\mathcal{C}_{\Theta_{(2)}}$, respectively. For both scenarios, we assume that the same Clayton copula family and Gamma and lognormal marginal distributions, although different distribution and copula parameters apply in the two scenarios. Scenario 1 leads to fixed model parameters, while Scenario 2 considers that the model parameters change when one considers data before and after the breakpoint, $b_{k \setminus k+1}$. Using maximum likelihood, we will evaluate and maximize the following objective function:

$$\Psi_{k \setminus k+1} = \psi(X_1) + \psi(X_2) - \psi(X),$$
 (1)

where $\psi(\cdot)$ is a function computed based on the regularized maximum log-likelihood of the available data with regard to the predefined copula family and marginal distributions.

Note that $\psi(X)$, first, employs MLE model parameters, Θ , based on the assigned data, X. The MLE method allows estimation of the marginal distribution parameters and the copula family parameters; MATLAB provides functions named fitdist and copulafit that accomplish this task. The regularized maximum log-likelihood function is obtained as follows:

$$\psi(X) = \sum_{i=1}^{n} \left(\log c_{\alpha} \left(F_{1}(x_{1}(i)|a,b), F_{2}(x_{2}(i)|\mu,\sigma) \right) + \log f_{1}(x_{1}(i)|a,b) + \log f_{2}(x_{2}(i)|\mu,\sigma) \right) - \frac{\lambda}{s_{1}^{2} + s_{2}^{2}},$$
(2)

where n is the length of the input bivariate time series, X; $c_{\alpha} = \frac{\partial^2 C_{\alpha} \left(u_1 = F_1(x_1|a,b), u_2 = F_2(x_2|\mu,\sigma)\right)}{\partial u_1 \partial u_2}$

is the copula probability density function; $u_1 = F_1(x_1|a,b)$ and $u_2 = F_2(x_2|\mu,\sigma)$ are marginal cumulative distribution functions; $f_1(x_1|a,b)$ and $f_2(x_2|\mu,\sigma)$ are marginal probability density functions; s_1 and s_2 are marginal sample standard deviations. To avoid overfitting, marginal variance regularization is applied and $\lambda \geq 0$ is the regularization parameter. The order of magnitude of the marginal variances, together with λ , influences the role of regularization, which is discussed in Section 2.3.

Note that $\Psi_{k \setminus k+1}$, as defined, is the regularized maximum log likelihood difference between the likelihood function based on data sub-segments divided at the breakpoint, $b_{k \setminus k+1}$, and the likelihood function based on the entire unsegmented drifts, et. We calculate $\Psi_{k \setminus k+1}$ for every possible breakpoint and then select an optimal breakpoint $a_k \circ b_{k \cdot k+1}$ as follows:

$$k_1^* = \underset{k}{\operatorname{argmax}} \Psi_{k \setminus k+1}, \quad (3)$$

and we also ensure that $\Psi_{k_1^*\backslash k_1^*+1}>0$. If every Ψ returns a negative value, it means that further segmentation has no advantage. In this case, the greedy algorithm stops the segmentation search and we go to the *Return* stage

Figure 4 shows 999 Ψ values computed with k=100. The maximum Ψ value occurs for k=600. Based on this result, we divide the distance segments at the breakpoint, $b_{600\setminus 601}$. These resulting sub-segments are shown in Figure 5.

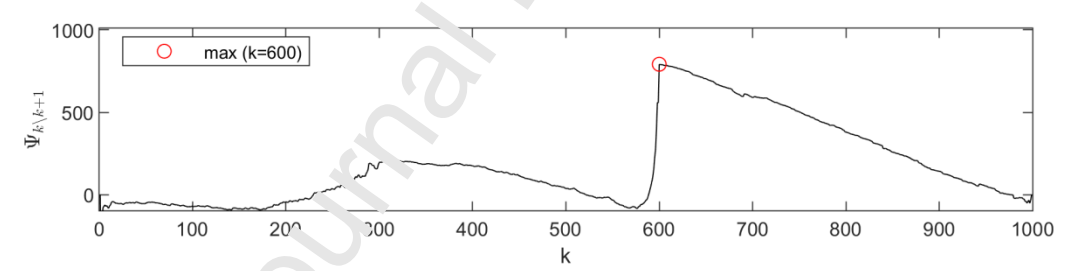


Figure 4. Calculated objective function Ψ for the benchmark data at the first iteration.

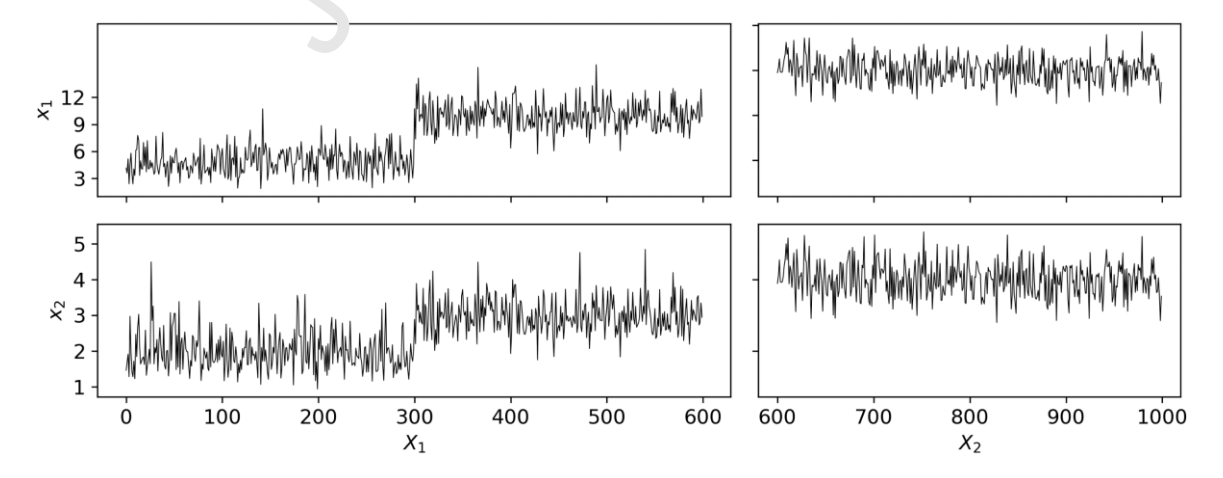


Figure 5. Sub-segments generated by the first identified breakpoint, $b_{k_1^* \setminus k_1^* + 1} = b_{600 \setminus 601}$.

2.1.2 Iteration 2

After the previous (first) iteration, what we have are new segmented data sets, $X_1 = [\mathbf{x}_1, ..., \mathbf{x}_{600}]^T$ and $X_2 = [\mathbf{x}_{601}, ..., \mathbf{x}_{1,000}]^T$. Thus, the number of current segments, K = 2, and the number of new breakpoints possible is now 998. Again, we compute Ψ for every possible breakpoint and ultimately select a new optimal breakpoint, $b_{k_2^* \setminus k_2^* + 1}$. We reject the new breakpoint and terminate the greedy algorithm if all Ψ values have a negative value. An additional termination condition is invoked in Iteration 2 and beyond, if the identified optimal breakpoint is not from the current last sub-segment. This is because our goal with the greedy search algorithm is to find and use only the last stationary sub-segment to be representative of the most likely series for the near future. Therefore, if further segmentation cannot be continued on the current last sub-segment, we terminate the search. On the other hand, if there is a breakpoint, $b_{k_2^* \setminus k_2^* + 1}$, within the last sub-segment (in Iteration 2, the last segment $= X_2$) and $\Psi_{k_2^* \setminus k_2^* + 1} > 0$, we accept this new breakpoint and continue the iteration with the new segmented data sets, $X_1 = [\mathbf{x}_1, ..., \mathbf{x}_{600}]^T$, $X_2 = [\mathbf{x}_{601}, ..., \mathbf{x}_{k_2^*}]^T$, and $X_3 = [\mathbf{x}_{k_2^* + 1}, ..., \mathbf{x}_{1,000}]^T$. Otherwise, the algorithm moves to what we refer to as the *Return* stage.

2.1.3 Iteration 3+

We repeat the procedure above until any one of the termination conditions: 1) all $\Psi < 0$; 2) k^* does not match an index number in the last sure-segment. After we terminate this iterative greedy search, the algorithm moves to the final \tilde{k} er and stage.

2.1.4 Return

As final output, the algorithm returns the current last segment as the identified optimal data sub-segment. We denote this data set as X_{opt} . Note that $X_{opt} \subseteq X$.

Figure 6 shows calculated 993 T values for the benchmark data set at Iteration 2. The maximum value occurs at k=310 on the first segment. This means that we have reached the second termination condition. We stop the iterations and send the current last subsegment $X_2 = \left[\mathbf{x}_{601}, \dots, \mathbf{x}_{1,000}\right]^T$ to the *Return* stage. As a result, the identified optimal data set, $X_{opt} = X_2 = \left[\mathbf{x}_{601}, \dots, \mathbf{x}_{1,000}\right]^T$.

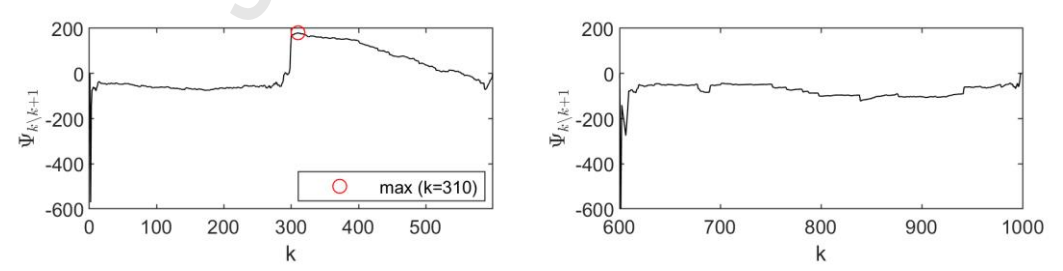


Figure 6. Calculated objective function Ψ for the benchmark data at the second iteration.

The GCS algorithm can be generalized to any d-dimensional multivariate data set, $X = [\mathbf{x}_1, ..., \mathbf{x}_N]^T \in \mathbb{R}^{N \times d}, \mathbf{x}_i = (x_1(i), ..., x_d(i))$. Let $f_i(x_i|\theta_i)$ be the probability density function and $u_i = F_i(x_i|\theta_i)$ be the cumulative distribution function for variable, x_i . Multivariate copulas can be denoted as $C_\Theta = C_\alpha(u_1, ..., u_d)$, where $\Theta = (\alpha, \theta_1, ..., \theta_d)$. The regularized maximum log-likelihood function for multivariate data, X, is given as:

$$\psi(X) = \sum_{i=1}^{N} \left(\log c_{\alpha}(u_{1}, \dots, u_{2}) + \sum_{j=1}^{d} \log f_{j}(x_{j} | \theta_{j}) \right) - \frac{\lambda}{\sum_{j=1}^{d} s_{j}^{2}}.$$
 (4)

Figure 7 shows the general GCS algorithm flowchart based on the preceding discussion.

Greedy Copula Segmentation

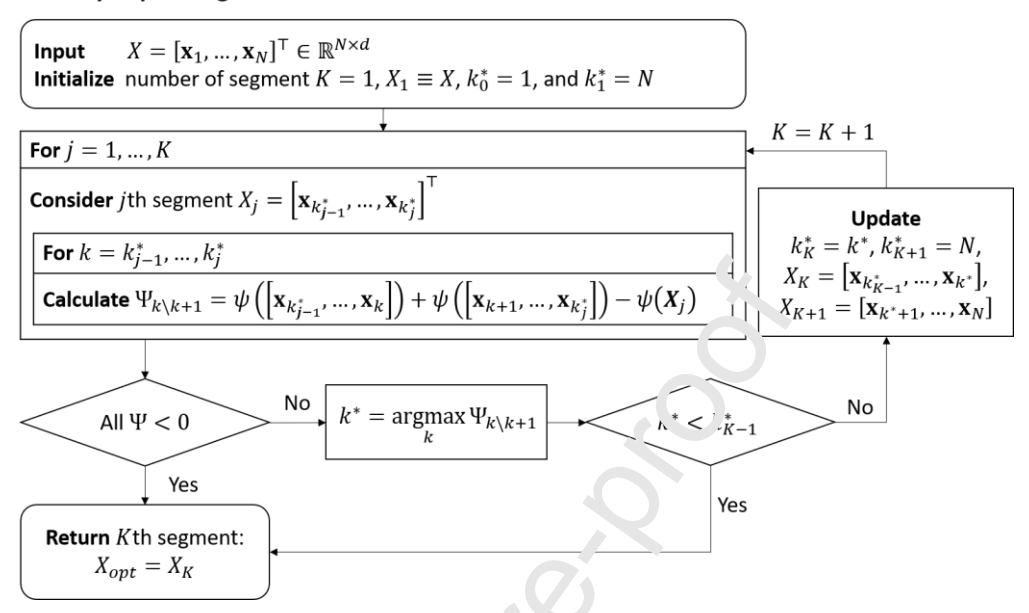


Figure 7. Greedy Copula Segmentation (GCS) algorithm flowchart.

2.2 Climate Change Adaptation with the Lanchmark Data

We are interested in attempting a climic schange adaptation strategy using GCS assuming that the bivariate data in Figure 1 Coscribe climate parameters of interest. Suppose the benchmark data set, X, represe; is a 100 year-long set of observations with 10 records per year. Let us first consider a cituation where only the first 40 year-long set (400 samples) represent the base data. The 'raditional approach would develop the base joint copula, $C_{\Theta_{(0)}}$ using all the base data, but or optimal approach will use the GCS-identified optimal data only for near-future projections. Then, such a derived joint distribution will be used for any risk assessment until the new data are obtained, or the existing data set from 40 years is updated. Suppose this distribution is updated in increments corresponding to 10-year cycles. Again, the traditional approach would use all of the now 50 year-long set (500 samples) to obtain a new updated version of the joint copula, $C_{\Theta_{(1)}}$, but our optimal approach will again use the GCS-identified optimal data only. The procedure can be repeated every 10 years and two different joint copulas can be developed based on the two different approaches (traditional vs. GCS).

To highlight the comparative prediction performance of the two approaches, we compute log-likelihoods for m update cycles, each of 10-year length as follows:

Two different joint copulas,
$$C_{\Theta_{trad_m}}$$
 and $C_{\Theta_{opt_m}}$, are derived using the base data and the same number of new 10 year data undates \mathbf{x}_i $i=1$, m_i is applied to calculate the log

Two different joint copulas, $C_{\Theta_{trad_m}}$ and $C_{\Theta_{opt_m}}$, are derived using the base data and the same number of new 10-year data updates, \mathbf{x}_i , $i=1,\ldots,n_m$, is applied to calculate the log-likelihood in Equation 5. As such, the calculated log-likelihoods are fair performance measures to allow comparisons between traditional and GCS approaches. The copula and

corresponding approach that yields a higher likelihood when the new data are included is more accurate than the alternative. In other words, the traditional and GCS approaches offer models based on the base data that are then used to assess how well they perform against different lengths of update cycle data increments; relative comparison is possible using Equation 5.

A general formulation can be defined using t_{base} (the base period) and t_{cyc} (the period covered in each update cycle). At cycle m, the traditional approach uses all the data collected from the beginning until $t_{base}+m\cdot t_{cyc}$ to update the distribution, whereas GCS-CCA uses X_{opt_m} for the corresponding distribution. Note that each t_{cyc} -long data update can be used to evaluate predictive performance. Figure 8 shows a diagram summarizing the two different approaches with the formulation as presented.

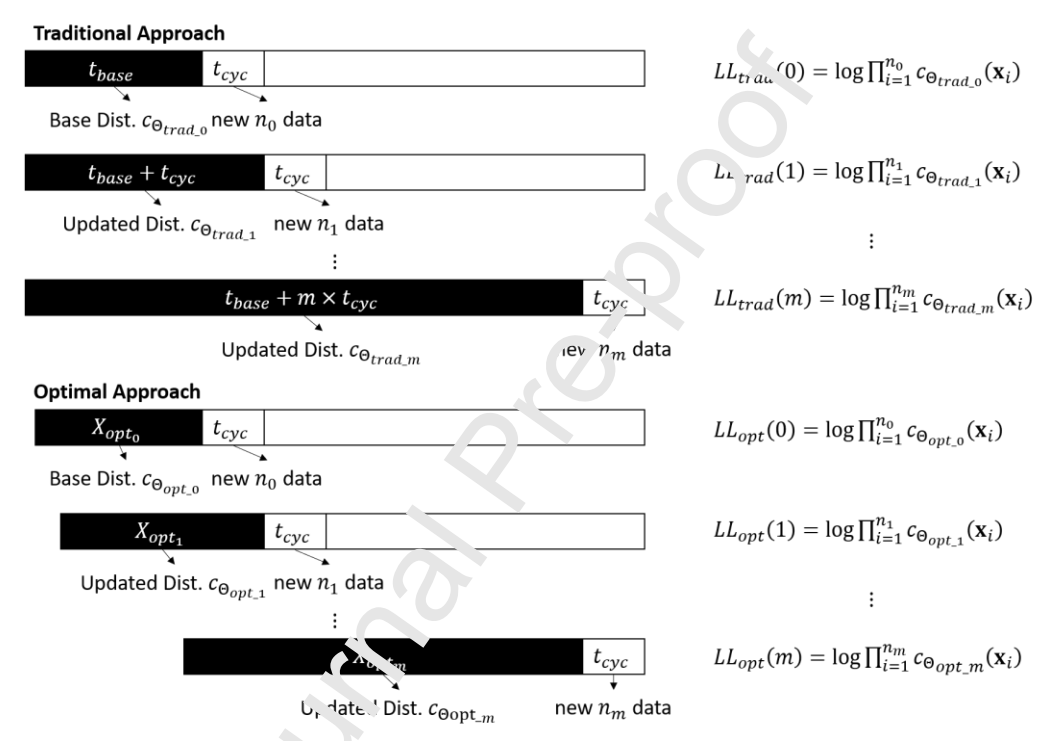


Figure 8. Traditional and optimal GCS approaches for climate change adaptation.

The predictive performance is evaluated 6 times since we choose, each time, the first 400 samples as the base data and add 100 new samples in each update cycle. To allow overall predictive performance comparisons between the traditional CCA and GCS-CCA, we compute the mean predictive log-likelihood difference ratio, M, over all the update cycles:

$$M(\%) = \frac{1}{6} \sum_{i=0}^{5} \frac{LL_{opt}(i) - LL_{trad}(i)}{|LL_{trad}(i)|} \times 100.$$

We repeat this entire procedure 10 times by synthetically generating (using random sampling) a new benchmark data set each time. Figure 9 shows the mean and min-max error bars of M(%) with different regularization parameter choices, λ . We can easily confirm that GCS-CCA outperforms traditional CCA for sufficiently large parameters, λ , that range between 5 and 100. One can also directly evaluate the influence of λ ; for lower values of λ , GCS-CCA performs better than traditional CCA. However, a lower-valued regularization parameter implies more overfitting and then its performance is not better than that with traditional CCA. Higher-valued regularization parameter levels restrict segmentation and

then GCS-CCA is basically the same as traditional CCA. It is only for intermediate-valued λ values where GCS-CCA with associated segmentation is seen to be superior.

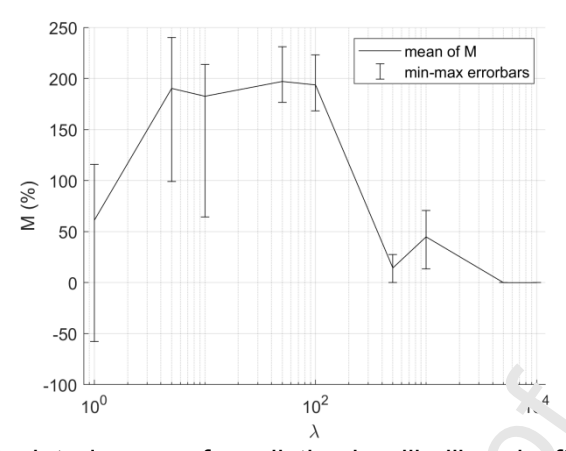


Figure 9. Calculated mean of predictive log-likelihood of ference ratio, M, over all update cycles with different choices for regularization parameter, λ .

2.3 Regularization Parameter Selection

GCS-CCA leads to more accurate prediction than traditional CCA if we can select the proper regularization parameter, λ . Its value can be chosen by trial and error, using prior knowledge, or using a principled method, such as Eayesian or Akaike information criterion or cross validation (Hallac et al., 2019). In yone al, one needs a sufficiently high value for λ because this parameter directly influences the extent of segmentation that results. Too high a value for λ results in no segmentation, which is then equivalent to traditional CCA; on the other hand, a low value for λ leads to overfitting, which means that GCS will select a very short recent sub-segment as the or in all data. Then, the joint distribution of the underlying variables is overly fitted to this small amount of data. As we can see from Equation 4, the order of magnitude of the magnitude of the magnitude, together with λ , influences the role of regularization. In Figure 9, v e systematically evaluate the role of λ in assessing model quality. Results indicate that CCS-CCA's effectiveness is hurt by overfitting and inferior performance when λ value are low. Also, the results with traditional CCA are virtually the same as GCS-CCA when a values are too high. Overall predictive performance of GCS-CCA is an improvement over traditional CCA over a considerably wide range of λ values from 5 to 100. This later finding suggests too a lower sensitivity of λ on the benchmark data; if some moderate amount of regularization is imposed with GCS-CCA, superior performance over traditional CCA is assured.

3. Experiments with Drought Patterns in CCA

Several hydroclimate variables – e.g., precipitation, air temperature, soil moisture, etc. – simultaneously affect drought scenarios. Indices or scores derived from univariate and multivariate drought indicators that are in turn based on individual or multiple hydroclimate variables have been developed to characterize and quantify drought conditions. Such scores are included in a drought index, and drought index time series can then be used to describe the input data for drought severity-duration-frequency (SDF) analysis.

For an experiment involving real data analysis and application of GCS-CCA, we collected climate data – representing monthly total precipitation and a monthly average of daily average temperature data – from the Global Historical Climatology Network-Monthly

(GHCN-M) Version 3 dataset (Lawrimore et al., 2011). Various types of drought indices were calculated using open-source software originally developed by National Integrated Drought Information System (NIDIS), National Centers for Environmental Information (NCEI), and National Oceanic and Atmospheric Administration (NOAA) (Adams, 2017). The collected climate variables and calculated drought indices cover the geospatial extent: latitude 24.5625 ~ 49.354168 (degrees north), longitude -124.6875 ~ -67.020836 (degrees east), and raster dimensions, (latitude, longitude, time) = (38, 87, 1466). One grid cell near the Austin, Texas area was selected for a regional case study. Figure 10 shows the area covered by the selected grid cell.

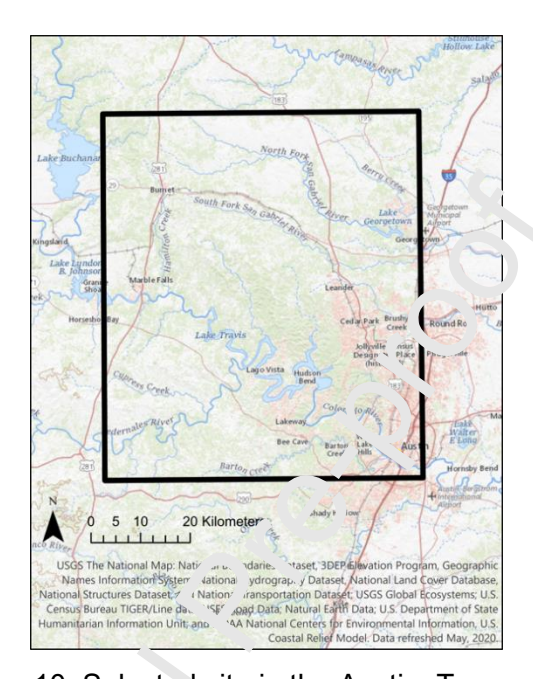


Figure 10. Selected site in the Austin, Texas area.

Among various drought indices the Standardized Precipitation Evapotranspiration Index utilizing a Gamma distribution with a 3-month scale (SPEI_G3), developed by Vincente-Serrano et al., 2010 was selected to serve as an indicator of drought events. This selection is justified because studies have shown that SPEI performs better in drought assessments under a global warming transport by combining the multi-scalar character with the capacity of involvement of tempera are effects on droughts (Hao and Singh, 2015; Tan et al., 2015; Homdee at al., 2016). Detailed information about SPEI and its calculation can be found in the studies by Vincente-Serrano et al., 2010; Begueria et al., 2014; Hameed et al., 2018.

Figure 11 shows the calculated SPEI_G3 time series, denoted by Z, that is obtained for the period, December 1896 to February 2017. The Thornthwaite equation is used to derive potential evapotranspiration (PET) from air temperature data.

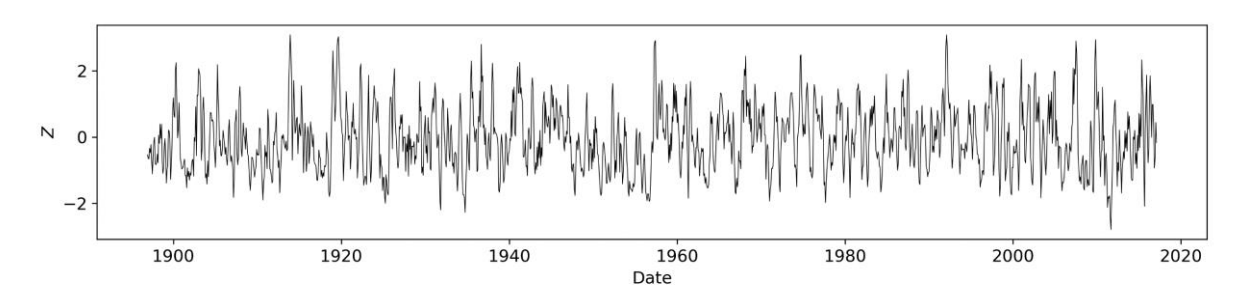


Figure 11. Calculated standardized precipitation evapotranspiration index utilizing Gamma distribution and 3-month scale (SPEL G3) time series.

This study describes the entire procedure that starts with preparing a bivariate drought pattern time series and proceeds to a final predictive performance evaluation. We provide a step-by-step guide that can be used for not only several types of drought events but also for other extreme climate events and applications that have a similar problem setting and data structure.

3.1 Bivariate Drought Pattern Time Series

To apply GCS, first, we extract drought events from the selected drought index time series using a predefined truncation level. The overall concept of how we define a drought event and its associated duration, d_i , and severity, s_i is illustrated in Figure 12. In this study, drought duration and severity are selected for the analysis since they have been widely used for drought severity-duration-frequency (SDF) analysis. A similar concept can be applied to other climate data time series.

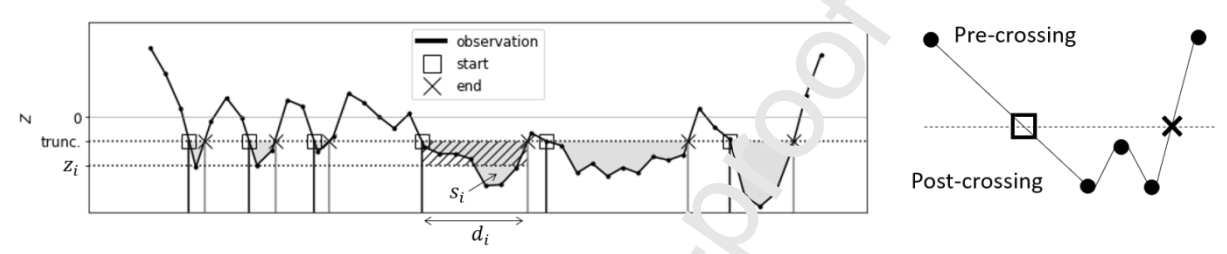


Figure 12. A concept diagram showing definitions of drought event duration, severity, and equivalent intensity, along with indications of pre-crossing and a post-crossing.

Our definition is a modified version of the very evjevich (1967) theory of run model. We define the start and end of a drought event by interpolating pre-crossing and post-crossing data points given the data. In this manner for any drought event, i, the drought duration, d_i defined as the time difference between the start and end – is real-valued. Then, the absolute value of the integral area between the under time series and the selected horizontal truncation level from the start to the end of the event is defined as the drought severity, s_i . An equivalent drought index value z_i , associated with drought event, i, is easily calculated. Mathematically, $z_i = s_i/d_i$, which is sometimes referred to as drought intensity (Cavus and Aksoy, 2020). This drought index when considered at a constant level over the duration of the event leads to an area based severity that is equivalent to the observed value, s_i , for the same event. This is clear too from Figure 12. To be clear, we refer to z_i as an equivalent intensity.

Suppose we extract N drought events from the given drought index time series. Then, the input data, $X = [\mathbf{x}_1, \dots, \mathbf{x}_N] \in \mathbb{R}^{N \times 2}$, where $\mathbf{x}_i = (d_i, s_i)$. Each data point can now be considered as data obtained at the start of corresponding drought event. We can now apply GCS-CCA to the input drought data.

Vincente-Serrano et al., 2010 defined various ranges of SPEI values as associated with different intensities of droughts: light drought (-0.5 to -0.99), moderate drought (-1.0 to -1.49), severe drought (-1.5 to -1.99), and extreme drought (-2.0 \leq). In the present study, a truncation SPEI level of -0.5 is selected so as to include even the mildest drought conditions in our assessment. Accordingly, a total of 143 drought events with associated duration and severity (or equivalent intensity) are extracted from the SPEI_G3 time series.

Figure 13 shows the duration, severity, and equivalent intensity values considering all the drought events extracted over the period of measurements (1896-2017) in the selected Austin, Texas region. Average and standard deviation values are shown for the data and are

also shown using a 5-year moving window. The moving average and standard deviation variation clearly indicate non-stationary characteristics in the drought pattern. Figure 14 shows scatter plots of the collected data, showing two of the drought-related variables at a time. Based on similar assumptions in past studies, exponential and gamma distributions are selected as marginal probability distributions for duration and severity, respectively. The Gumbel copula family is selected to model the pairwise dependence structure for these two variables (Zelenhasic and Salvai,1987; Hao and Singh, 2013).

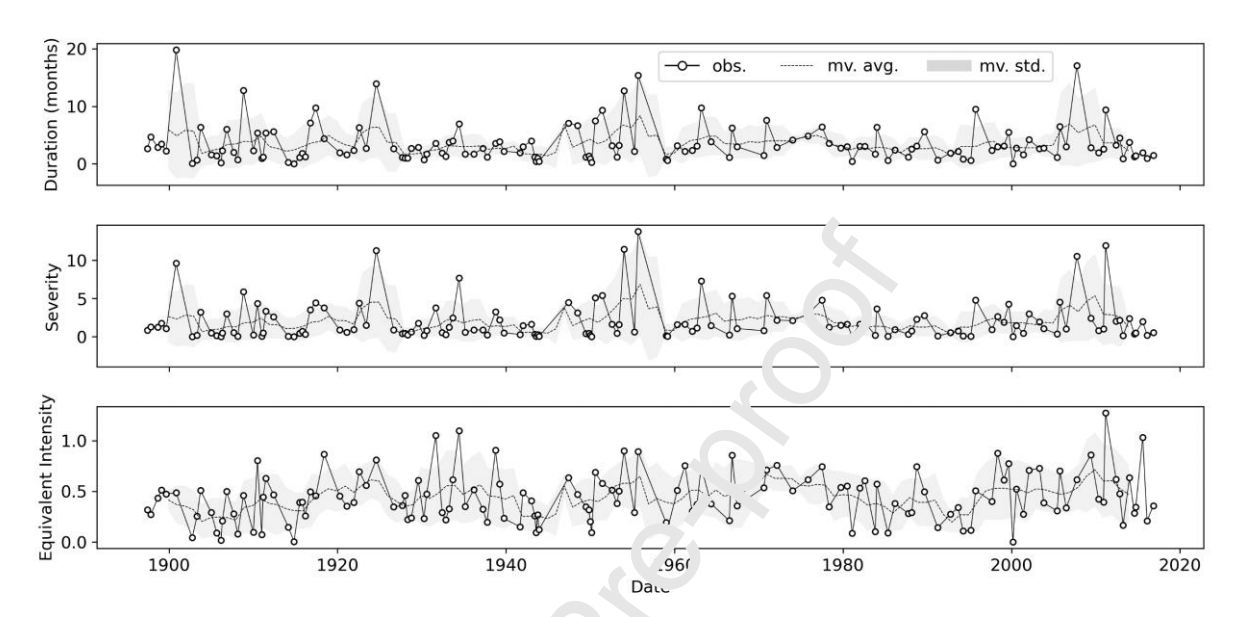


Figure 13. Duration, severity, and equ valent intensity values from 143 extracted drought events, using a -0.5 \(\text{\text{\cuteff}}\) notation level with the SPEL G3 data.

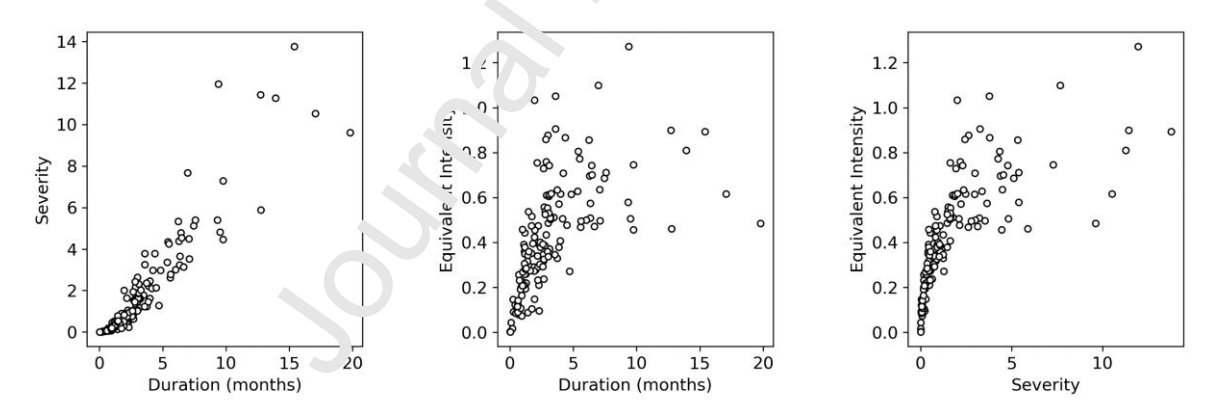


Figure 14. Pairwise scatter plots showing duration, severity, and equivalent intensity for all the drought events in the data set.

We begin by considering only the initial 20-year data as base data and then include 10-year increments as update cycles in projections to be used in possible climate change adaptation, where the GCS-CCA approach seeks to optimize justified use of only the most recent data. The overall input data covers about 120 years (December 1896 to February 2017) and, thus, there are 10 predictive performance evaluations of GCS-CCA versus a traditional that ignores non-stationary trends.

Figure 15 shows results summarized in terms of the mean predictive log-likelihood difference ratio, M, over the update cycles considered. As before, M is defined as follows:

$$M(\%) = \frac{1}{10} \sum_{i=0}^{9} \frac{LL_{opt}(i) - LL_{trad}(i)}{|LL_{trad}(i)|} \times 100.$$

We can easily verify that GCS-CCA outperforms traditional CCA for sufficiently large λ values that range from 110 to 180. This finding suggests that GCS-identified optimal data sub-segments explain near-future drought patterns better than when all of the historical observed data are used. Figure 15 shows that lower values λ lead to overfitting while higher values makes GCS-CCA essentially equivalent to traditional CCA. Pre-processing of the data and applying an appropriate regularization parameter is recommended for such analyses.

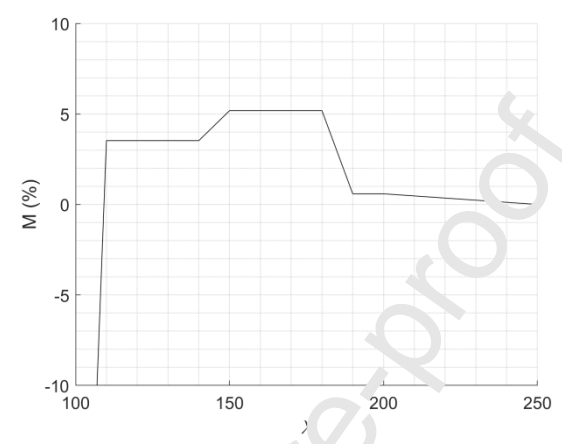


Figure 15. Calculated mean of predictive loc-likelihood difference ratio, M, over all update cycles for the drought data with diff are nt choices for regularization parameter, λ.

All the computations were executed in NATLAB on a 64-bit Microsoft desktop computer with 6 Intel i7-9750H CPUs at 2.60 G' 12 and 32 GB of RAM. Figure 16 compares CPU times for 10 predictive performance evaluations using the traditional CCA and the proposed GCS-CCA for the drought patterns data and with different λ (regularization) values. Because GCS-CCA requires additional computation using the greedy segmentation algorithm, which attempts to select the optimal segments out of a combinatorically large pool, Figure 16 shows that GCS-CCA requires a greater amount of CPU time than traditional CCA. Nevertheless, GCS-CCA is still a fairly light computational exercise easily undertaken on a common desktop computer that was used in the experiments and, while also considering all of the update cycles, it allows easy and efficient prediction of drought patterns over a window covering the next 10 years. We can see the role of the regularization parameter again; CPU time is less when λ is higher because increased regularization restricts the segmentation and requires less computation.

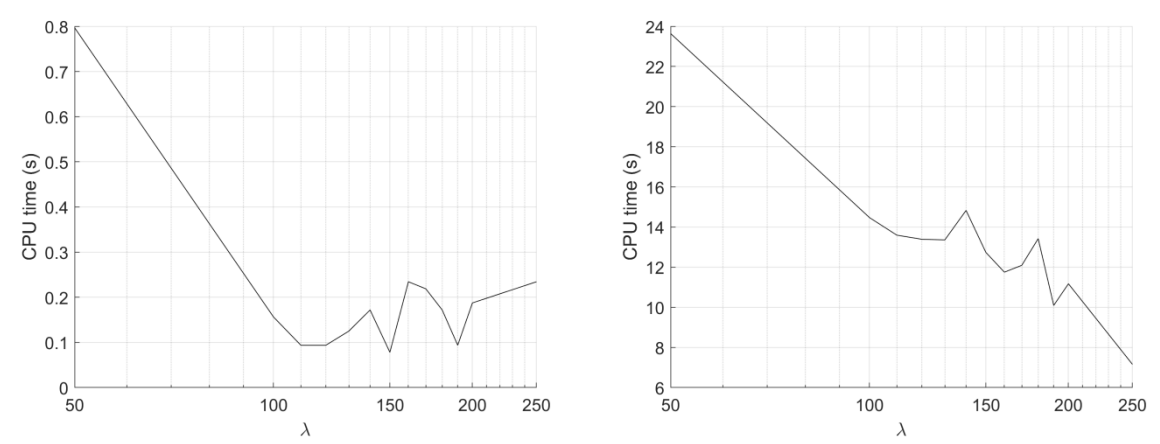


Figure 16. CPU time for climate change adaptation with the drought patterns data and different λ values: traditional approach (left) and Greedy Cerula Segmentation (right)

4. Discussion

Patterns in extreme climate time series will continue to change due to inherent non-stationary characteristics as well as constantly changing anthropogenic influences. Figures 9 and 15 have clearly shown what can be learned by considering climate as a piecewise stationary process in decision-making for near-fiture prediction. Accurate data-driven prediction provides objective information to rolleginakers to aid in addressing disaster risk reduction (DRR) and climate change adaptation (CCA). A quantitative assessment of socioeconomic damage mitigation strategies based on GCS application can aid in CCA policy amendments; such strategies will depend or collaboration with domain experts from various disciplines including civil and environmental engineering, geosciences, public affairs, management, and economics.

We have offered a validation of the proposed GCS-CCA methodology, highlighting its advantages in the context of single site drought events. GCS-CCA can easily be extended to apply to other types of disasters that are characterized by multiple climate variables. Since GCS-CCA is formulated to work with multivariate data, analysis for multiple sites and/or for greater spation overage can readily be undertaken. By utilizing multivariate copulas, GCS offers the mathematical tractability to enable its use in general multivariate non-stationary time series. Human-induced variables that influence disaster risks can as well be incorporated along with climate-related variables for comprehensive near-future DRR and CCA.

One limitation of the proposed GCS-CCA methodology is the need for pre-processing of the data. The selection of regularization parameters in the assessment has been briefly discussed in Section 2.3. This selection choice will introduce more complexity when a high-dimensional space of variables must be considered. In addition, some basic domain knowledge is required to establish appropriate marginal distributions and copula families for the variables. If these are not available or otherwise known, model selection using criteria such as AIC, BIC, or cross-validation is unavoidable. To allow even more generalized formulation, non-parametric kernel density functions and non-parametric copula dependence structures may also be employed. Such options and decisions would then be model-free; however, interpretation of results should be done with care since nonparametric approaches can lead to greater error in extreme values when input data are insufficient.

5. Conclusions

In this work, we have extended the Greedy Gaussian segmentation (GGS) algorithm developed by Hallac (2019) by allowing multivariate Gaussian distributions in the copula definition; we refer to this extended approach as greedy copula segmentation (GCS). Our extension is well-suited for use with climate data since many climate-related variables are non-Gaussian and non-stationary. Based on the wide coverage of different dependence structures possible with the copula family choice, it is expected that GCS could be used in various applications that involve long sequences of multivariate time series data. We have explained GCS, iteration by iteration, so as to offer an accessible description of the greedy algorithm.

Using a synthetic data set as well as an observed drought data set, we have shown that GCS can optimize future projections for possible use in climate change adaptation. Climate change adaptation needs to rationally consider periodic updates of the joint distribution of climate variables by focusing on patterns seen in extreme climate events. We introduce the notion of considering trends in any climate parameter as oes understood by defining a piecewise process consisting of several stationary sub-segments to represent the data. In such a piecewise stationary representation, the latest (most recent) stationary sub-segment (whose length must be iteratively established, using maximum likelihood with regularization) can predict most rationally and precisely any near-future patterns in the extreme climate that are to be expected. The proposed GCS approact identifies the most informative data sampled from the latest stationary sub-segment; it it eractively evaluates the benefit of further segmentation on the last segment. By doing so, the algorithm greedily searches for the optimal last segment of input data.

We show that the GCS-identified optic all data produce better predictive performance for possible climate change adaptation by incistrative examples using a benchmark synthetic data set as well as a real 120-year or night-related data set from Austin, Texas. GCS-CCA shows superior predictive performance for the non-stationary benchmark problem. For the real-world application, we collect create index time series data and extract the bivariate drought event (duration and severity) ata. The GCS-CCA results suggest that the proposed approach can rationally uncore changing climate patterns in the time series and can produce accurate near-future projection for adaptation plans compared to more traditional approaches that seek to use it in going or complete historical data sets. The outlined framework can be easily communicated in policymakers who are non-scientific experts. We expect that our model will reduce the going between academia, researchers, and data scientists on the one hand and policymakers on the other. We also expect that the GCS-CCA framework can help towards achieving the Sendai framework goals by offering a rational approach to risk reduction in the face of non-stationary climate hazards.

References

- Adams, J. (2017). climate_indices, an open source Python library providing reference implementations of commonly used climate indices. URL: https://github.com/monocongo/326climate%7B%5C %7Dindices.
- Aminikhanghahi, S. and Cook, D. J. (2017) A Survey of Methods for Time Series Change Point Detection. *Knowledge and Information Systems*. 51 (2), 339–367.
- Bandyopadhyay, N. et al. (2020) Drought mitigation: Critical analysis and proposal for a new drought policy with special reference to Gujarat (India). *Progress in Disaster Science*. 5, 100049.
- Beguería, S. et al. (2014) Standardized precipitation evapotranspiration index (SPEI) revisited: parameter fitting, evapotranspiration models, tools, datasets and drought monitoring. International journal of climatology. 34 (10), 3001–3023.
- Carrão, H. et al. (2016) Mapping global patterns of drought risk: An empirical framework based on sub-national estimates of hazard, exposure ε nd vulnerability. *Global Environmental Change*, 39, 108-124.
- Cavus, Y. & Aksoy, H. (2020) Critical drought severity/intensity-ouration-frequency curves based on precipitation deficit. Journal of hydrology. 584, 724312–.
- Cid, A. et al. (2016) Long-term changes in the frequency, nter sity and duration of extreme storm surge events in southern Europe. *Climate Dynamics*. 46 (5), 1503–1516.
- Dai, A. (2013) Erratum: Increasing drought under global warming in observations and models. Nature climate change. 3 (2), 171–171.
- De Michele, C. & Salvadori, G. (2003) A Generalizer Pa. eto intensity-duration model of storm rainfall exploiting 2-Copulas. *Journal of Geophysical Research: Atmospheres*. 108 (D2), 4067–n/a.
- Djalante, R. and Lassa, S. (2019) Governing complexities and its implication on the Sendai Framework for Disaster Risk Recuction priority 2 on governance. *Progress in Disaster Science*. 2, 100010.
- Esling, P. and Agon, C. (2012) Time-caries data mining. *ACM Computing Surveys*. 45 (1), 1–34.
- Garcia Galiano, S. G. et al. (2015) A.s. ie sing Nonstationary Spatial Patterns of Extreme Droughts from Long-Term (Can-Resolution Observational Dataset on a Semiarid Basin (Spain). *Water (Pasal)*. 7 (10), 5458–5473.
- Genest, C. & Favre, A.-C. (200.) Everything You Always Wanted to Know about Copula Modeling but Were Afraid to Ask. *Journal of Hydrologic Engineering*. 12 (4), 347–368.
- Genest, C. et al. (2011) Estir nators based on Kendall's Tau in Multivariate Copula Models.

 **Australian and Few Zealand Journal of Statistics. 53 (2), 157–177.
- Hallac, D. et al. (2019) Greedy Gaussian segmentation of multivariate time series. *Advances in data analysis and classification*. 13 (3), 727–751.
- Hameed, M. et al. (2018) Apprehensive Drought Characteristics over Iraq: Results of a Multidecadal Spatiotemporal Assessment. Geosciences. 8 (2), 58.
- Hao, Z. & Singh, V. P. (2013) Entropy-Based Method for Bivariate Drought Analysis. *Journal of Hydrologic Engineering*. 18 (7), 780–786.
- Hao, Z. & Singh, V. P. (2015) Drought characterization from a multivariate perspective: A review. Journal of hydrology. 527, 668–678.
- Homdee, T. et al. (2016) A comparative performance analysis of three standardized climatic drought indices in the Chi River Basin, Thailand. *Agriculture and Natural Resources*. 50 (3), 211-219.
- Ishiwatari, M. and Surjan, A. (2019) Good enough today is not enough tomorrow: Challenges of increasing investments in disaster risk reduction and climate change adaptation. *Progress in Disaster Science*. 1, 100007.
- Izumi, T. et al. (2019) Disaster risk reduction and innovations. *Progress in Disaster Science*. 2, 100033.

- Jehanzaib, M. et al. (2020) Investigating the impacts of climate change and human activities on hydrological drought using non-stationary approaches. *Journal of Hydrology*, 588, 125052.
- Jehanzaib, M. et al. (2021) Reassessing the frequency and severity of meteorological drought considering non-stationarity and copula-based bivariate probability. *Journal of Hydrology*, 126948.
- Lawrimore, J. et al. (2011) Global Historical Climatology Network Monthly (GHCN-M), Version 3. DOI: https://doi.org/doi:10.7289/V5X34VDR.
- Lee, J. et al. (2020) Water-related disasters and their health impacts: A global review. *Progress in Disaster Science*. 5, 100123.
- Lee, T. & Ouarda, T. B. M. J. (2010) Long-term prediction of precipitation and hydrologic extremes with nonstationary oscillation processes. *Journal of Geophysical Research: Atmospheres.* 115 (D13).
- Li, J. et al. (2015) Evaluation of Nonstationarity in Annual Maximum Flood Series and the Associations with Large-scale Climate Patterns and Ht man Activities. *Water Resources Management*. 29 (5), 1653–1668.
- Liu, S. et al. (2019) Identification of the Non-stationarity of Floods Changing Patterns, Causes, and Implications. Water resources management. 33 (3), 939–953.
- Manuel, L. et al. (2018) Alternative Approaches to Develop En /ironmental Contours from Metocean Data. *Journal of Ocean Engineering and warine Energy*, 4(4).
- Mathier, L. et al. (1992) The Use of Geometric and Garma-Related Distributions for Frequency Analysis of Water Deficit. Stochas in Fydrology and Hydraulics: Research Journal. 6 (4), 239–254.
- Matsuoka, Y. & Rocha, E. G. (2021) The role of non-government stakeholders in implementing the Sendai Framework: A vev from the voluntary commitments online platform. *Progress in Disaster Scie*. 9, 100142.
- Mazdiyasni, O. et al. (2019) Heat wave 'nter.sity Duration Frequency Curve: A Multivariate Approach for Hazard and Attributio. Analysis. *Scientific reports*. 9 (1), 14117–14118.
- Mishra, A. K. & Singh, V. P. (2010) A review of drought concepts. *Journal of hydrology*, 391(1-2), 202-216.
- Nelsen, R. B. (2006) An Introduction to copulas by Roger B. Nelsen. 2nd ed. 2006. New York, NY: Springer New York
- Nystrup, P. et al. (2017) Long memory of financial time series and hidden Markov models with time-varying parameters. *Journal of Forecasting*, 36(8), 989-1002.
- Ouarda, T. B. M. J. & Charron, C. (2018) Nonstationary Temperature-Duration-Frequency curves. *Scientific Peuxs.* 8 (1), 15493–15498.
- Patel, S.S. et al. (2021) Delivering the promise of the Sendai Framework for Disaster Risk Reduction in fragile and conflict-affected contexts (FCAC): A case study of the NGO GOAL's response to the Syria conflict. *Progress in Disaster Science*. 10, 100172.
- Polunchenko, A. S. and Tartakovsky, A. G. (2012) State-of-the-Art in Sequential Change-Point Detection. *Methodology and Computing in Applied Probability*. 14 (3), 649–684.
- Reeves, J. et al. (2007) A Review and Comparison of Changepoint Detection Techniques for Climate Data. *Journal of Applied Meteorology and Climatology*. 46 (6), 900–915.
- Rigby, R.A. & Stasinopoulos, D.M. (2005) Generalized additive models for location, scale and shape. *Journal of the Royal Statistical Society: Series C (Applied Statistics)*, 54(3), 507-554.
- Rydén, T. et al. (1998) Stylized facts of daily return series and the hidden Markov model. Journal of applied econometrics, 13(3), 217-244.
- Saja, A. M. A., et al. (2019) Implementing Sendai Framework priorities through risk-sensitive development planning A case study from Sri Lanka. *Progress in Disaster Science*. 5, 100051.
- Saklar, A (1959) Fonctions de repartition a n dimensions et leurs marges. *Publications de l'Institut de Statistique de L'Universite de Paris 8*. pp. 229-231.
- Salvadori, G. (2004) Bivariate return periods via 2-Copulas. *Statistical Methodology*. 1 (1-2), 129–144.

- Salvadori, G. & De Michele, C. (2004) Frequency analysis via copulas: Theoretical aspects and applications to hydrological events. *Water Resources Research*. 40 (12).
- Schwalm, C.R. et al. (2017) Global patterns of drought recovery. *Nature*, 548(7666), 202-205.
- Sheffield, J. et al. (2012) Little change in global drought over the past 60 years. Nature. 491 (7424), 435–438.
- Shiau, J.-T. & Shen, H. W. (2001) Recurrence Analysis of Hydrologic Droughts of Differing Severity. *Journal of Water Resources Planning and Management*. 127 (1), 30–40.
- Singh, C. et al. (2021) Losses and damages associated with slow-onset events: urban drought and water insecurity in Asia. *Current Opinion in Environmental Sustainability*, 50, 72-86.
- Slater, L. J. et al. (2020) Nonstationary weather and water extremes: a review of methods for their detection, attribution, and management, Hydrol. Earth Syst. Sci. Discuss. [preprint], https://doi.org/10.5194/hess-2020-576, in review, 2020.
- Tan, C. et al. (2015) Temporal-Spatial Variation of Drought Inc cated by SPI and SPEI in Ningxia Hui Autonomous Region, China. *Atmosphere*. 6 (10), 1399–1421.
- Truong, C. et al. (2020) Selective review of offline change point a stection methods. *Signal Processing*. [Online] 167, 107299.
- Uchiyama, C. et al. (2021) Assessing contribution to the £ end ii Framework: Case study of climate adaptation and disaster risk reduction projects across sectors in Asia-Pacific (2015–2020). *Progress in Disaster Science*. 12, 100195.
- Van Loon, A. F. et al. (2016) Drought in the Anthroponen 3. Nature geoscience. 9 (2), 89–91.
- Vicente-Serrano, S. M. et al. (2010) A Multiscalar Drugot Index Sensitive to Global Warming: The Standardized Precipitation Proportion Index. Journal of climate. 23 (7), 1696–1718.
- Walz, Y et al. (2020) Monitoring progress of the Sendai Framework using a geospatial model: The example of people af ected by agricultural droughts in Eastern Cape, South Africa. *Progress in Disaster Science*. 5, 100062.
- Wang, Y. et al. (2015) A time-dependent drought index for non-stationary precipitation series. *Water Resources Marchement*, 29(15), 5631-5647.
- Wilkins, A. et al. (2021) Challenges and opportunities for Sendai framework disaster loss reporting in the United Strue Progress in Disaster Science. 10, 100167.
- Yevjevich (1967) An objective proach to definitions and investigations of continental hydrologic droughts. Hydrology Paper No. 23, Colorado State University, Fort Collins, Colorado.
- Yoo, J. et al. (2013) Bivariate diought frequency curves and confidence intervals: a case study using moninly rainfall generation. *Stochastic Environmental Research and Risk Assessment*. (271), 285–295.
- Yue, S. et al. (1999) The Jumbel mixed model for flood frequency analysis. *Journal of hydrology (Amsterdam)*. 226 (1), 88–100.
- Yue, S. (2001) A bivariate gamma distribution for use in multivariate flood frequency analysis. *Hydrological Processes*. 15 (6), 1033–1045.
- Zelenhasic, E. & Salvai, A. (1987) A method of streamflow drought analysis. *Water resources research*. 23 (1), 156–168.

- Greedy Copula Segmentation (GCS) is used to analyze non-stationary time series.
- Multivariate characteristics are episodically described using copula models.
- The use of GCS in plans for climate change adaptation is demonstrated.
- GCS allows judicious treatment of trends in data to make near-future predictions.

Taemin Heo: Conceptualization, Methodology, Original draft preparation. **Lance Manuel**: Writing, Reviewing, Editing, Funding Acquisition

Declaration of interests

oxtimes The authors declare that they have no known competing financial interests or personarelationships that could have appeared to influence the work reported in this paper.	al
☐ The authors declare the following financial interests/personal relationships which may be considered as potential competing interests:	